A simplified method to predict torsional effects on asymmetric seismic isolated buildings under bi-directional earthquake components

Raffaele Laguardia[a*], Carmen Morrone[a], Marco Faggella[a], Rosario Gigliotti[a]
[a] *Sapienza University of Rome, Department of structural and geotechnical engineering, Via Eudossiana 18, 00184 Rome, Italy.*

*corresponding author. Email: raffaele.laguardia@uniroma1.it

Keywords: Seismic Isolation, Torsional effects, Directionality effects, Accidental eccentricity, Linearized design.

ABSTRACT

The assessment of maximum displacement demand is a crucial point in the design of seismic isolating systems, in particular when the non linear behaviour of devices is modeled through visco-elastic equivalent schemes, as common in the design practice. Several phenomena influence the maximum demand assessment, among which the torsional and earthquake directionality effects can be of great impact. International codes use some formulations which allow to consider torsional effects, while the impact of the other phenomena is commonly assessed through time-history analyses. In this paper an innovative design method is developed based on an exact linear elastic formulation with response spectrum, which keeps in count both torsional and directivity effects considering natural and accidental eccentricity and by using the CQC3 (Menun and Der Kiureghian, 1998) as directional combination rule. The method models the seismic action through the response spectra of a set of natural recorded ground motions, properly oriented along their principal axes to assess the correct ratio between the horizontal components of spectral accelerations; thus accounting for the site-specific earthquake source, without the need to perform time-history analyses. A specific formalization of the dynamic problem is presented to emphasize the parameters which more affects the response (e.g. torsional factor, eccentricity, geometrical aspect ratio) and simplify its interpretation. Results obtained on two case studies are compared with time-history analyses to show the effectiveness of the procedure.

1 INTRODUCTION

The determination of maximum displacement demand on seismic isolation devices is a very important point to ensure both the effectiveness and affordability of seismic isolation systems (Kelly 1999; Warn and Whittaker 2004; Roussis et al. 2013). Underestimating the displacement capacity of devices can lead to the loss of their bearing capabilities resulting in heavy structural damages, yet excessive caution in demand estimation can lead to unjustified high costs of a system. Torsional and directionality effects and their mutual influence can have a major impact on the maximum displacement demand and the availability of effective prediction methods is a key point for effective seismic isolation design (Pant et al. 2013).

International building codes allow using linear and non-linear analysis methods for design and check of seismically isolated structures, both new and existing. As it is known, in general considering the non-linear behaviour of structures implies to keep in count several aspects and phenomena, such as those inherent to structural damage and non-ductile mechanisms (Calvi et al. 2002; Braga et al. 2009) infills-frame interaction (Mohammad et al. 2016) rebars bond-slip (Laterza et al. 2017 a,b; Caprili et al. 2018, Mohammad et al. 2018), complex structure-isolation interaction in dynamic

conditions due to devices nonlinearity (Braga et al. 2005), and complex dynamic behavior due to irregularity and eccentricity in conjunction with earthquake directionality (Faggella et al. 2018). These may lead to increased modelling and computational effort and likely uneasy interpretation of results, making nonlinear modelling approaches often unpractical for day-to-day design purposes by professional engineers. In particular, for base isolated structures, the development of reliable linear analysis methods that take into account torsional and directionality effects with reasonable accuracy would greatly simplify the design and proportioning process. In fact, an inherent simplification of seismic isolation systems relies in the fact that they are usually designed to obtain an elastic or almost elastic behaviour of the structural portion that they intend to protect, with nonlinearities concentrated in the devices, whose behaviour is easier to predict and control. This makes seismic isolation attractive compared to other techniques that often require the nonlinear behaviour assessment of the whole structure (Formisano et al. 2008; Dall'Asta et al. 2017; Morelli et al. 2017; Laguardia et al. 2017; Formisano and Massimilla 2018; Braga et al. 2019). In general, linear analyses through the use of a proper linearization procedure can be performed, provided that some applicability conditions are met, as requested by the main international codes (CEN 2004; NTC 2008; ASCE 2010; NTC 2018). Linearization procedures reproduce the nonlinear behaviour of devices through an equivalent lateral stiffness, K_{eq}, and an equivalent damping ratio, ζ_{eq}, so to determine the maximum displacement demand of the devices and the maximum force transmitted to the superstructure with linear analysis.

Torsion of buildings due to non-symmetric or non-regular distribution of stiffness is commonly described as "natural torsion" (Chopra and De la Llera 1996), while other torsional effects may occur due to several additional aspects, such as irregular distribution of masses, torsional earthquake input component, asymmetries due to constructive errors or other (Koren and Kilar 2011). These effects are commonly considered as "accidental torsion" (Chopra and De la Llera 1996). Usually, seismic isolation systems can be designed to minimize the "natural torsion" through a proper selection and distribution of stiffness. Nevertheless, uncertainties about the actual distribution of masses, presence of torsional components of motion or unexpected behaviour of isolating devices require to consider some accidental torsional effects. Normally, the accidental torsional effects are taken into account by using an "accidental eccentricity", by placing the centre of mass at a certain distance from its original position. In the main international codes (CEN 2004; NTC 2008; ASCE 2010; NTC 2018) this distance is taken as ± the 5% of the plan dimension of the building. Torsional effects can then be modelled by explicitly considering the accidental eccentricity in the model or, as an alternative, by applying an equivalent torque to the system. The first approach is more appropriate if the goal is to model the eccentricity due to uncertainties on mass distribution, while the second is more appropriate if the interest is in modelling the earthquake torsional component.

In the literature several works have been carried out on this topic and the discussion is still open (Nagarajaiah et al. 1993; Chopra and De la Llera 1996; Menun and Der Kiureghian 1998; Jangid and Kelly 2000; Ryan and Chopra 2004; Athanatopoulou 2005; Trombetti and Conte 2005; Tena-Colunga and Zambrana-Rojas 2006; Tena-Colunga and Escamilla-Cruz 2007; Trombetti et al. 2008; Palermo et al. 2013; Faggella et al. 2013, 2018; Basu et al. 2014; Wolff et al. 2014; Faggella 2014a, 2014b; Basu et al. 2015; Basu and Giri 2015; Faggella et al. 2017). In particular, (Chopra and De La Llera 1996) carried out a study on the dynamic response of several single-storey and multi-storey structures subjected to a rotational component of the earthquake, evaluating the effectiveness of the method proposed by ASCE 7 (ASCE 2010) for the assessment of effects related to accidental torsion. The rotational component of the earthquake input has been calculated on the basis of recorded horizontal Ground Motions (GMs). The results obtained were in good agreement with the ASCE 7 method. Jangid and Kelly (2000) performed an analytical study on the effects of torsion for base isolated systems, providing a description of physical parameters that influence most the structural response. They

propose a comparison with the ASCE 7 formulation and common rules of combination (Absolute, SRSS, CQC). Palermo et al. (2013) conducted a careful analysis on the dynamic equation of motion of torsionally coupled elastic systems and developed a simplified method for predicting the maximum rotation of the system. Wolff et al. (2014) analysed the formulation proposed by ASCE 7 to evaluate the torsional amplification factor also through a comparison with experimental tests. Given the relevance of the results obtained, they suggested a change to the ASCE 7 simplified method. Basu et al. (2014) proposed an alternative approach for assessing the effects of the single torsional component, excluding the uncertainties related to the masses distribution in order to find a relationship with accidental eccentricity. Torsional effects related to the earthquake rotational component were evaluated analyzing the response of a structure subjected to concurrent rotational and translational time histories; they concluded proposing a different accidental eccentricity value, according to the response of the structure to the torsional component of the earthquake. Faggella (2014a, b) and Faggella and et al. (2017) proposed a number of "Graphic-Dynamic" methods for predicting maximum torsional displacements, of which the Mohr Circle response spectrum analysis is particularly suited to base isolated systems and one-way asymmetric systems in general. A more comprehensive Graphic-Dynamic method is formulated by Faggella et al. (2018) incorporating torsion and earthquake directionality under a common graphic rational prediction rule, applicable also to two-ways asymmetric systems.

Beside torsional effects, a number of other works addressed the influence of bi-directional earthquake. Warn and Whittaker (2004) showed that, for both near fault or far fault earthquake, the formulations available in the codes did not provide an accurate estimate of the maximum design displacement if equivalent linear methods were used. Several other works followed on this topic and a complete review is given by Pant et al. (2013) who state that linear equivalent methods provide good accuracy in determination of maximum displacement demand in almost all cases. Further, even though it is beyond the objectives of this work, it should be noted that several works were carried out on near-fault effects, emphasizing the relevance to the maximum displacement determination (Jangid and Kelly 2001; Dicleli and Buddaram 2007; Lu and Lin 2009). For both near fault and far fault events, it should be stressed that the uncertainty regarding the actual seismic demand is one of the critical aspects in the maximum displacement determination. In this sense, all the existing methods based on linear analyses do not consider this aspect. Therefore, there is currently no method that allows the designer to carry out analyses by varying the seismic demand, adapting it to the specific characteristics of the site through appropriate earthquake source studies and therefore modeling the seismic action with natural ground motion records.

The scope of this work is to provide an analysis method based on linear elastic analyses, allowing to determine the maximum displacement demand of seismic isolation systems by explicitly considering the torsional and bi-directional earthquake loading effects and representing the seismic action through the response spectra of natural ground motions instead of traditional code spectra. Through an appropriate definition of an asymmetric dynamic system, this paper highlights the influence of the structural properties (expressed through the torsional factor Ω_s) on the maximum displacement amplification due to torsional effects, emphasizing the limitations of the currently available international codes methods. Further, this displacement amplification is investigated considering a concurrent two-directional earthquake loading by using the CQC3 directional combination (Menun and Der Kiureghian 1998). The advantages of the CQC3 in assessing the maximum displacement are shown by considering the critical angle of incidence for each structural configuration and the influence of the ratio between the spectral accelerations adopted for the two considered input directions. Given the possibility of the CQC3 rule to account for different ratio of spectrum components, the proposed methodology can be used representing the seismic input through the response spectra of natural ground motions properly oriented along their principal axes, thus allowing to consider with good accuracy and completeness, the

uncertainties related to seismic action in an explicit way. A comparison with time-history analyses performed on two case studies, shows how the proposed methodology allows a very close estimate of the maximum displacement retaining the design-oriented practicality and reduced modeling and computational effort, requiring only an appropriate selection and modification of natural ground motions.

2 EARTHQUAKE RESPONSE OF TORSIONALLY COUPLED STRUCTURES

2.1 Uni-directional earthquake loading

The problem of an asymmetric isolated structure subjected to mono-directional earthquake loading is investigated highlighting the theorethical aspects of the structural response for torsionally coupled systems.

Torsional effects depend primarily on the mass and stiffness distribution of the system, and on the characteristics of the seismic action. One of the most significant parameters governing the seismic behaviour of buildings is the torsional factor Ω_s, which represents the ratio between the purely translational and purely torsional modal periods of the structure. The dynamic problem of a system with two degrees of freedom and subjected to a single-component earthquake is formalized to explicit the definition and the influence of Ω_s. In Fig. 1 a generic asymmetric dynamic system is represented, with an eccentricity e_x between the centre of mass *G* and the centre of stiffness *K*. Such eccentricity likely results in a torque acting on the system, as shown in Fig. 2. By considering the centre of mass as the origin of the system and the two degrees of freedom, u_y and u_θ, as the translation in the y-direction and rotation about the z-axis, respectively, with the assumption of equal stiffness and *equal masses* of the system along X and Y directions, rigid diaphragm behaviour and small rotations u_θ, the dynamic problem is governed by the following equations:

$$\mathbf{0} = \boldsymbol{F_m} + \boldsymbol{F_e} = \boldsymbol{M\ddot{u}} + \boldsymbol{Ku} \tag{1}$$

$$\boldsymbol{u} = \begin{Bmatrix} u_y \\ u_\theta \end{Bmatrix} \tag{2}$$

$$\boldsymbol{F_m} = m \begin{bmatrix} 1 & 0 \\ 0 & \rho^2 \end{bmatrix} \begin{Bmatrix} \ddot{u}_y \\ \ddot{u}_\theta \end{Bmatrix} \tag{3}$$

$$\boldsymbol{F_e} = K_y \begin{bmatrix} 1 & e_x \\ e_x & e_x^2 + \rho_y^2 \end{bmatrix} \begin{Bmatrix} u_y \\ u_\theta \end{Bmatrix} \tag{4}$$

where $\boldsymbol{F_m}$ is the vector of inertial forces, $\boldsymbol{F_e}$ is the vector of elastic forces, $\boldsymbol{M}$ is the mass matrix, $\boldsymbol{K}$ is the stiffness matrix, m is the total translational mass of the system, I_p is the rotational mass, $\rho = \sqrt{I_p / m}$ is the mass gyrator, K_y is the total translational stiffness of the system, K_θ is the total torsional stiffness, $\rho_y = \sqrt{K_\theta / K_y}$ is the stiffness radius in the y-direction.

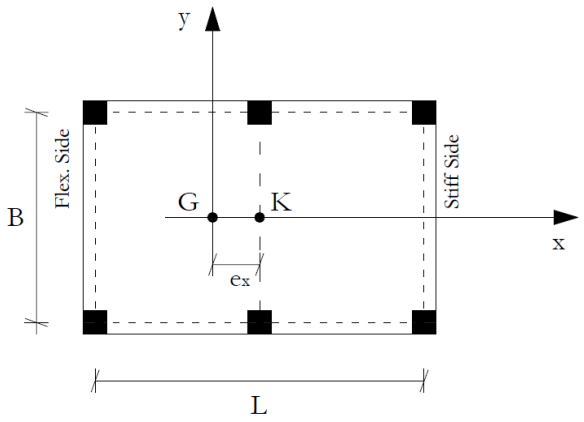

Fig. 1 Asymmetric dynamic system with eccentricity between the centre of mass *G* and the centre of stiffness *K*

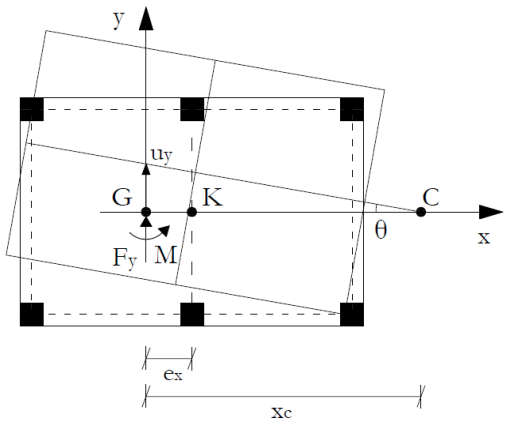

Fig. 2 Representation of seismic forces acting on a generic asymmetric dynamic system with eccentricity between the centre of mass *G* and the centre of stiffness *K*

By dividing and multiplying the second row by ρ, the equations of motions (Eq. 4) can be expressed as follows (Faggella 2014a)

$$\boldsymbol{I}\ddot{\boldsymbol{u}}_{\boldsymbol{\rho}} + \frac{1}{m}\boldsymbol{K}_{\boldsymbol{p}}\boldsymbol{u}_{\boldsymbol{\rho}} = \boldsymbol{0} \tag{5}$$

$$\frac{1}{m}\boldsymbol{K}_{\boldsymbol{p}} = \omega_y^2 \begin{bmatrix} 1 & \varepsilon_x \\ \varepsilon_x & q^2 \end{bmatrix} \tag{6}$$

where: ω_y is the circular frequency of the translational mode for an idealized non-eccentric structure, $d = \sqrt{e_x^2 + \rho_y^2}$ is the coupled stiffness radius, $q = d/\rho = \sqrt{\varepsilon_x^2 + \Omega_s^2}$ is the normalized coupled stiffness radius, $\varepsilon_x = e_x/\rho$ is the dimensionless eccentricity, $\Omega_s = \rho_y/\rho$ is the torsional factor of the non-eccentric system and $u_\rho = [u_y \quad u_\theta \rho]^T$ is the vector of equivalent translational degrees of freedom.

From the theoretical model shown above, it is clear that the structural response is strictly related to the Torsional factor Ω_s, which is a characteristic parameter of the uncoupled structure. Generally, when Ω_s>1 structure is defined as torsionally-rigid, while when Ω_s<1 the structure is called torsionally-flexible.

In order to study the free vibration with no damping of the structural system described through Eq. 5 and Eq. 6, the modal properties of the system are obtained by solving the following eigenproblem

$$\left[\frac{1}{m}\boldsymbol{K_p} - \boldsymbol{I}\omega^2\right]\boldsymbol{\phi} = \mathbf{0} \tag{7}$$

where $\boldsymbol{\phi_i}$ are the eigenvectors solution to the problem and ω_i are the eigenfrequencies.

The circular frequencies of the i-mode, ω_i, and the dimensionless frequencies of the i-th mode, α_i, can be expressed as follows

$$\alpha_{1,2} = \frac{\omega_{1,2}^2}{\omega_y^2} = \frac{1}{2}(1+q^2) \mp \sqrt{\left(\frac{1-q^2}{2}\right)^2 + {\varepsilon_x}^2} \tag{8}$$

Alternatively, the periods of the two modal shapes, T_i, can be expressed as follows

$$\begin{aligned} T_1 &= \frac{T_L}{\sqrt{\frac{1}{2}(1+q^2) - \sqrt{\left(\frac{1-q^2}{2}\right)^2 + \varepsilon_x^2}}} \\ T_2 &= \frac{T_L}{\sqrt{\frac{1}{2}(1+q^2) + \sqrt{\left(\frac{1-q^2}{2}\right)^2 + {\varepsilon_x^2}^2}}} \end{aligned} \tag{9}$$

where T_L is the period of the uncoupled system.

The eigenvectors are obtained imposing the condition that at least one component of each vector is unitary

$$\boldsymbol{\phi_i} = \begin{bmatrix}\phi_{i1}\\ \phi_{i2}\end{bmatrix} \tag{10}$$

$$\boldsymbol{\phi_1} = \begin{bmatrix}\frac{\varepsilon_x}{\alpha_1 - 1}\\ 1\end{bmatrix} \tag{11}$$

$$\boldsymbol{\phi_2} = \begin{bmatrix}\frac{\varepsilon_x}{\alpha_2 - 1}\\ 1\end{bmatrix} \tag{12}$$

Using the same notations, the modal contribution factors, $\overline{M_i}$ can be expressed as follows

$$\begin{aligned} \bar{M}_1 &= \frac{1}{1 + \left(\frac{\alpha_1 - 1}{\varepsilon_x}\right)^2} \\ \bar{M}_2 &= \frac{1}{1 + \left(\frac{\alpha_2 - 1}{\varepsilon_x}\right)^2} \end{aligned} \tag{13}$$

Once the properties are known of the free vibration system in terms of modal shapes and frequencies, the structural earthquake response can be determined by using the response spectrum method with the SRSS or CQC modal combination rules.

In the case of SRSS the maximum displacement of the center of mass,is determined as

$$u_{G,SRSS} = \sqrt{\sum_{i=1}^{2} u_{G,i}^2} = \sqrt{u_{G,1}^2 + u_{G,2}^2} \tag{14}$$

$$u_{G,i} = S_{d_i}(T_i)\overline{M_i} \tag{15}$$

where: $u_{G,i}$ is the maximum displacement of the center of mass of the i-th modal shape, T_i is the period of the i-th modal shape, $S_{di}(T_i)$ is the spectral displacement for a period T_i.

Alternatively, the maximum displacement of the center of mass can be determined through the CQC combination rule

$$u_{G,CQC} = \sqrt{\sum_{i=1}^{2}\sum_{j=1}^{2} \rho_{ij}\, u_{G,i} u_{G,j}} = \sqrt{u_{G,SRSS}^{\ 2} + 2\cdot\rho_{12} u_{G,1max} \cdot u_{G,2max}} \tag{16}$$

where ρ_{ij} is the correlation factor between i-th and j-th mode expressed as a function of damping coefficients ξ_i and ξ_j and modal frequencies ratio $\beta_{ij} = \frac{\omega_i}{\omega_j} = \frac{T_j}{T_i}$:

$$\rho_{ij} = \frac{8\sqrt{\xi_i \xi_j}\left(\xi_i + \beta_{ij}\xi_j\right)\beta_{ij}^{\frac{3}{2}}}{\left(1-\beta_{ij}^2\right)^2 + 4\xi_i\xi_j\beta_{ij}\left(1+\beta_{ij}^2\right) + 4(\xi_i^2 + \xi_j^2)\beta_{ij}^2} \tag{17}$$

The maximum displacement of a generic point P of the system can be determined through CQC and SRSS combination rules once the position of the rotation centre C_i of the i-th mode, $x_{c,i}$ is defined, and the displacement of point P for each mode, $u_{p,i,}$

$$x_{c,i} = \frac{e_x}{1-\alpha_i} \tag{18}$$

$$u_{P,i}(x) = -S_{di}\overline{M_i}\left(\frac{x}{x_{C_i}} - 1\right) \tag{19}$$

$$u_{P,SRSS}(x) = \sum_i \sqrt{u_{P,imax}^2(x) + u_{P,jmax}^2(x)} \tag{20}$$

$$u_{P,CQC}(x) = \sum_i \sqrt{u_{P,imax}^2(x) + u_{P,jmax}^2(x) + 2\cdot\rho_{ij} u_{P,imax}(x)\cdot u_{P,jmax}(x)} \tag{21}$$

where: x is the coordinate of the generic point P.

2.2 Maximum displacement amplification factor

In order to determine the influence of the torsional effects, the maximum displacement ratio between eccentric and non-eccentric system, namely the torsional amplification factor R_w, is defined as

$$R_w = \frac{u_{ec}}{u_{Nec}} \tag{22}$$

Where u_{ec} is the displacement of the eccentric system, obtained through Eq. 20 or Eq. 21 and u_{Nec} is the displacement of the non-eccentric system.

Fig. 3 shows the amplification factors for an eccentric system subjected to a single-component earthquake. The maximum amplification factors of the stiff and flexibleside of the system, as depicted in Fig. 1, are shown with solid and

dashed lines, respectively. The results obtained through SRSS and CQC modal combinations are compared with the amplification factors provided in some international codes, such as NTC (2008) and ASCE (2010) and in Wolff et al. (2014).

$$\delta_{EC} = 1 + \frac{e_x}{r_x^2} y \tag{23}$$

$$\delta_{A7} = 1 + y\left(\frac{12e_x}{b^2 + d^2}\right) \tag{24}$$

$$\delta_{A7m} = 1 + \frac{y}{\Omega_s^2}\left(\frac{12e_x}{b^2 + d^2}\right) \tag{25}$$

where: δ_{EC} is the amplification factor obtained through NTC (2008), δ_{A7} is the amplification factor obtained through ASCE (2010) and δ_{A7m} is the amplification factor proposed by Wolff et al. (2014), r_x^2 is the torsional radius of the system, *y* is the distance from the center of stiffness, *b* and *d* are the plan dimension of the system.

It can be notice that simplified formulations provide conservative estimates of maximum displacement at the stiff side, with the exception of torsionally-flexible systems (Ω_s<1) with e_x=5% and ζ<10%. As for the flexible side, all the simplified formulations underestimate the maximum displacements in the case of torsionally-rigid structures (Ω_s>1). Specifically, the method proposed by NTC (2008) and by Wolff and Constantinou (2014) provide lower amplification factor than method proposed herein in almost all the analysed cases, while the method proposed by ASCE (2010) only for 1<Ω_s<1.5 and ζ<10%.

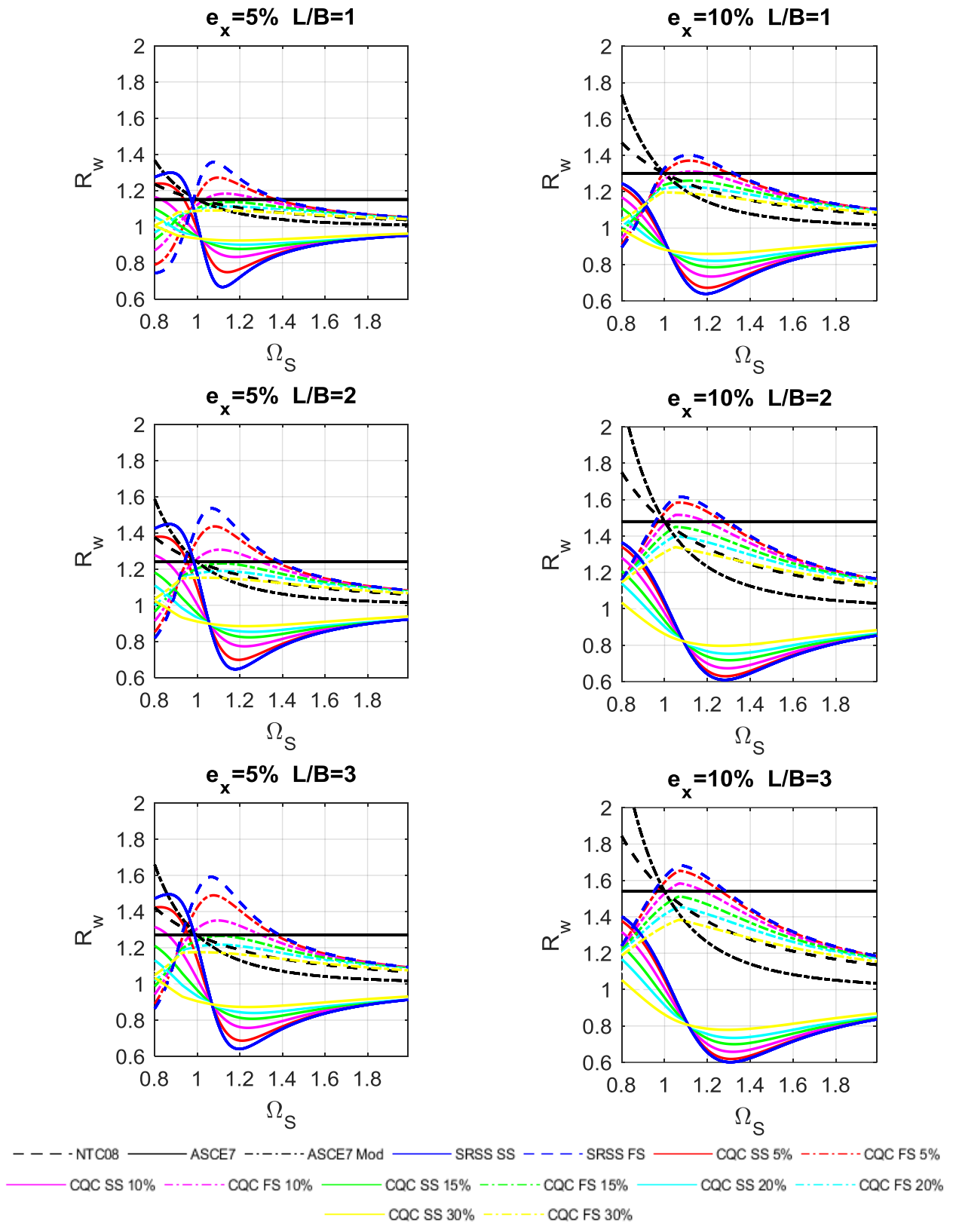

Fig. 3 Amplification factor R_W for eccentric systems subjected to single-component earthquake, evaluated with CQC combination for the stiff side (SS) and the flexible side (FS) for several values of equivalent damping ξ

2.3 Bi-directional earthquake loading

For practical design purposes, all the three seismic component, two horizontal and one vertical, should be taken into account. The combination rules commonly suggested in the international codes are the SRSS or, as an alternative, the 100-30 combination rule (Wilson et al. 1981). These combination rules don't allow to take explicitly into account the directionality effects and the actual ratio between the two seismic component.

In order to consider these effects, the CQC3 combination rule (Menun and Der Kiureghian 1998) is adopted here. This combination rule take into account the incidence angle of the earthquake on the building, θ, and the ratio of principal seismic components in the horizontal direction, γ. The maximum effect, R_{max}, is obtained by combining the maximum effects obtained through simple single-direction dynamic analyses for each direction of loading j, R_j, then combined through the following expressions

$$R_{\max} = \sqrt{\left(R_1^2 + R_2^2 + R_3^2\right) - \left(1-\gamma^2\right)\left(R_1^2 - \frac{1}{\gamma^2}R_2^2\right)\sin^2\theta + 2\left(\frac{1-\gamma^2}{\gamma}\right)R_{12}\sin\theta\cos\theta} \tag{26}$$

$$\gamma = S_{2i}/S_{1i} \tag{27}$$

where: R_m is the response obtained through Eq. 21 for the m-th component of the earthquake, R_{ml} is the cross term of the response between m-th and l-th direction as defined in (Menun and Der Kiureghian 1998) and S_{mi} is the spectral ordinate of m-th direction for the i-th period.

As an alternative, Eq. 26 can be expressed, as suggested by Menun and Der Kiureghian (1988), as follows

$$R = \sqrt{(R_1^2 + \gamma^2\tilde{R}_2^2 + R_3^2) - (1-\gamma^2)(R_1^2 - \tilde{R}_2^2)\sin^2\theta + 2(1-\gamma^2)\tilde{R}_{12}^2\sin\theta\cos\theta} \tag{28}$$

where R_{ml} and R_m are the response obtained by considering the l-th component of the earthquake acting along the m-th direction (i.e. $R_2 = \gamma\tilde{R}_2$ and $R_{12} = \gamma\tilde{R}_{12}$)

In general, the angle that maximizes the response is unknown, however, by differentiating Eq. 28 with respect to theta, it is possible to identify the critical angle, θ_{cr}, for which each effect is maximized, in the following way

$$\theta_{cr} = 0.5\tan^{-1}\left[\frac{2R_{12}}{R_1^2 - R_2^2}\right] \tag{29}$$

*It should be stressed that the γ coefficient is intended to be constant between the two horizontal components in Eqs. 27-29. Therefore, the assessment of such coefficient is straightaway if code spectra are used, while some assumptions need to be made for the assessment of such coefficient by using the spectra of natural recorded GMs, as it is discussed later in the numerical examples of section §4. As an alternative, some rules for the general case of different spectral shape may be found in (Smeby and der Kiureghian 1985; López and Torres 1997).*When two-directional earthquake loading is considered, the eccentricity should be taken into account in two directions, namely e_x and e_y shown in Fig. 4(a). Ryan and Chopra (2004) showed how this system can be reduced to a system with a single resulting eccentricity $e'_x = \sqrt{e_x^2 + e_y^2}$ through a rotation of the reference system, as shown in Fig. 4(b). The other dynamic properties of the system are not affected by this rotation, in the hypothesis that the isolating system stiffness is the same in both directions. Thus, the two-way dynamic system of Fig. 4(a) can be solved as a single-way dynamic system with equivalent one-way eccentricity e'_x through the procedure and the expressions described in the previous paragraph.

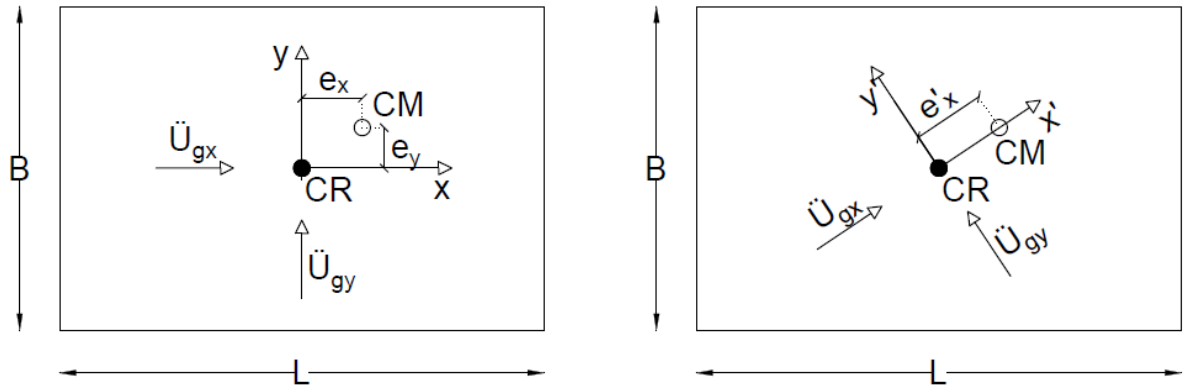

Fig. 4 Dynamic system with two-ways plan eccentricity with earthquake loading acting along x' and y'; single-way eccentric system with earthquake acting along the x and y directions.

By using the equivalent single-way eccentric system defined in Fig. 4, the displacement of the system with the CQC3 rule can be determined through Eq. 28. In order to assess the maximum demand on isolators, the resultant displacement is needed. Herein, such maximum demand is determined as the resultant of the two maximum displacement obtained along two orthogonal direction (e.g. u_x and u_y), assessed by considering the same angle of incidence, θ, for both.

In Fig. 5 are shown the R_w values calculated as the ratio between the maximum resultant displacement of the eccentric system subjected to two-components input and the maximum displacement of the idealized non-eccentric system subjected to single-component input for different values of the eccentricity, e_x, and different values of the maximum ratio between input components, γ. The trends are very similar to the ones obtained through monodirectional analyses, with a slight amplification on the stiff side for the torsionally-flexible systems ($\Omega_s<1$) and on the flexible side for torsionally-rigid systems ($1<\Omega_s<1.4$). The absolute values of R_w are sensibly higher, as an example for ζ=10%, L/B=1 and e_x=5%, the amplification factor is about 1.15 for monodirectional earthquake (see Fig. 3), while in the same conditions it assume values from 1.32 (γ=0.2) to 1.64 (γ=1) by considering bi-directional earthquake (Fig.5).

It should be observed that the high difference between bi-directional and monodirectional analyses is partially due to the assessment of the resultant displacement of two non contemporary maximum effects, even if assessed by considering the same angle of incidence, θ. In this regard, Clough and Penzien (1993), by using a probabilistic approach, suggest to amplify the results of monodirectional analyses by a factor of 1.12 (for γ=0.85) and 1.18 (for γ=1), providing lower maximum displacement in respect to those obtained herein

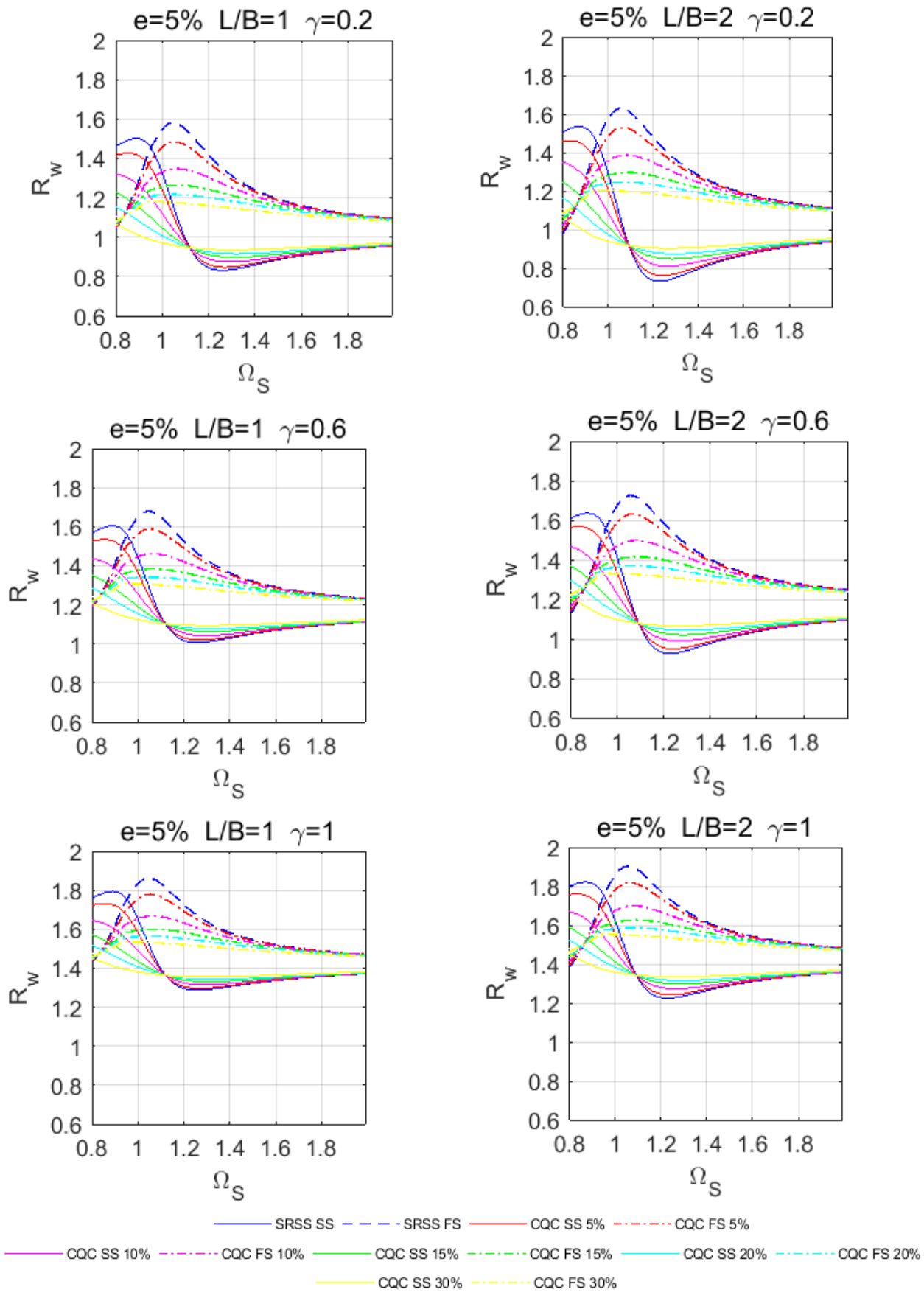

Fig. 5 Amplification factor R_W for eccentric systems subjected to bi-component earthquake, evaluated with CQC3 combination for the stiff side (SS) and the flexible side (FS) and several values of equivalent damping ξ

3 PROPOSED METHOD FOR MAXIMUM DISPLACEMENT DETERMINATION

The results described in section §2.2 and §2.3 point out that simplified methods available in the main international codes may not yield an accurate estimate of torsional effects for both single-direction and two-directions earthquake loading. In general, Time History (TH) dynamic analyses allow to highlight such inconsistencies and to improve the maximum displacement determination, however, performing TH analyses is not often viable in practical design conditions. Therefore the need emerged to develop a design method based on elastic linear analyses with an explicit modeling of the system eccentricity, which can comprehensively keep into account the torsional effects and the different ratio of input components, to correctly estimate the displacement amplifications due to two-direction earthquake loading.

To this goal, the method proposed herein can provide an improved demand estimate while retaining the use of the CQC3 combination rule, as discussed in section §2.3, joined with a representation of seismic action through response spectra of natural ground motions. This can provide a realistic estimate of the ratio between input components and allows to keep into account the specific seismic characteristics of the site, thus overcoming the limitations of design code spectra (Somerville 1998). Overall the method can yield a reliable assessment of maximum displacement including a higher level of information and model variables, yet retaining the simplicity of elastic linear analyses without the need to perform computationally intensive TH analyses.

3.1 GMs selection and determination of ground motions principal directions

The GMs records selection has a great impact on the final displacement computation, as described in the scientific literature in a number of available approaches for selecting and scaling ground motions records (Baker and Allin Cornell 2006; Baker and Cornell 2006; Faggella et al. 2013; Kohrangi et al. 2016; Faggella et al. 2016; Morelli et al. 2018). Nevertheless, there is no commonly recognized optimum method and, in general, the most commonly recommended strategy is to choose on a case-by-case basis, depending on the different design objectives. To correctly apply the proposed method, beside the GMs compatibility with earthquake source magnitude-distance and spectrum matching rules, it is of great interest to highlight some aspects regarding the assessment of the ratio between GMs components, or rather about the γ ratio to be used in Eq. 28. As known, the GMs are recorded according to two arbitrary axes, commonly positioned alongside east-west and north-south directions. The ground motion incidence angle at a certain site is unknown and then, in general, the two records are correlated to each other. This means that the use of ground motions "as-recorded" is inappropriate to determine the correct γ ratio. This problem was firstly analyzed by Penzien and Watabe (1974) who proposed to manipulate the records in order to determine the principal direction, defined as the direction where the correlation between the two components is null, in analogy with what commonly done for the stress states.

Limiting the interest to the two horizontal components, the principal directions are the directions along which, once the two horizontal records are projected, the correlation of the two histories is null (Rezaeian and Der Kiureghian 2010):

$$\rho_{a_1(t),a_2(t)} = \frac{\int_{t_1}^{t_2} a_1(t)a_2(t)dt}{\sqrt{\int_{t_1}^{t_2} a_1(t)^2 dt \int_{t_1}^{t_2} a_2(t)^2 dt}} \tag{31}$$

where ρ is the correlation factor, $a_i(t)$ is the acceleration of the i-th component at time t, t_j are the extremes of the time interval analysed.

The two horizontal components projected on the principal axes are defined as "principal" and "intermediate" (in the assumption that the "minor" component is vertical, as likely for the most cases).

3.2 Maximum displacement determination procedure

On the basis of what already shown about the structural response computation and ground motions selection, the maximum displacement of an isolating system considering torsional effects can be determined through the procedure depicted in Fig. 6, according to the following steps:

Step 1 - Definition of the isolation system:

Calculation of the normalized coupled stiffness radius, q, and the dimensionless eccentricity, ε_x, by the means of translational and rotational masses (m, I_ρ), translational and rotational stiffness (K_y, K_θ) and system eccentricity ($e'_x=\sqrt{e_x^2+e_y^2}$) as described in Section §2.1

Step 2 – Modal analysis of the system:

Determination of the modal periods, T_i, the modal participation factors, $\overline{M_i}$, and the rotation centres, $x_{c,i}$, of each modal shape through Eq. 9, Eq. 13 and Eq. 18, respectively.

Step 3 – Ground motions selections and principal direction:

Selection of a ground motions set and determination of principal direction as described in section §3.1. Determination of the spectral accelerations, $S_{d,k}(T_i)$, and the $\gamma_{,k}$ ratios the between principal and intermediate components for each ground motion.

Step 4 – Modal response:

Determination of the response due to the mode i for the earthquake acting along the direction h, $u_{p,ih}$, through Eq. 19.

Step 5 – Critical angle:

Determination of θ_{cr}, for the considered effect through Eq. 29.

Step 6 – Maximum displacement:

Determination of maximum displacement, $R_{max,k}$, for the k-th GM through Eq. 28.

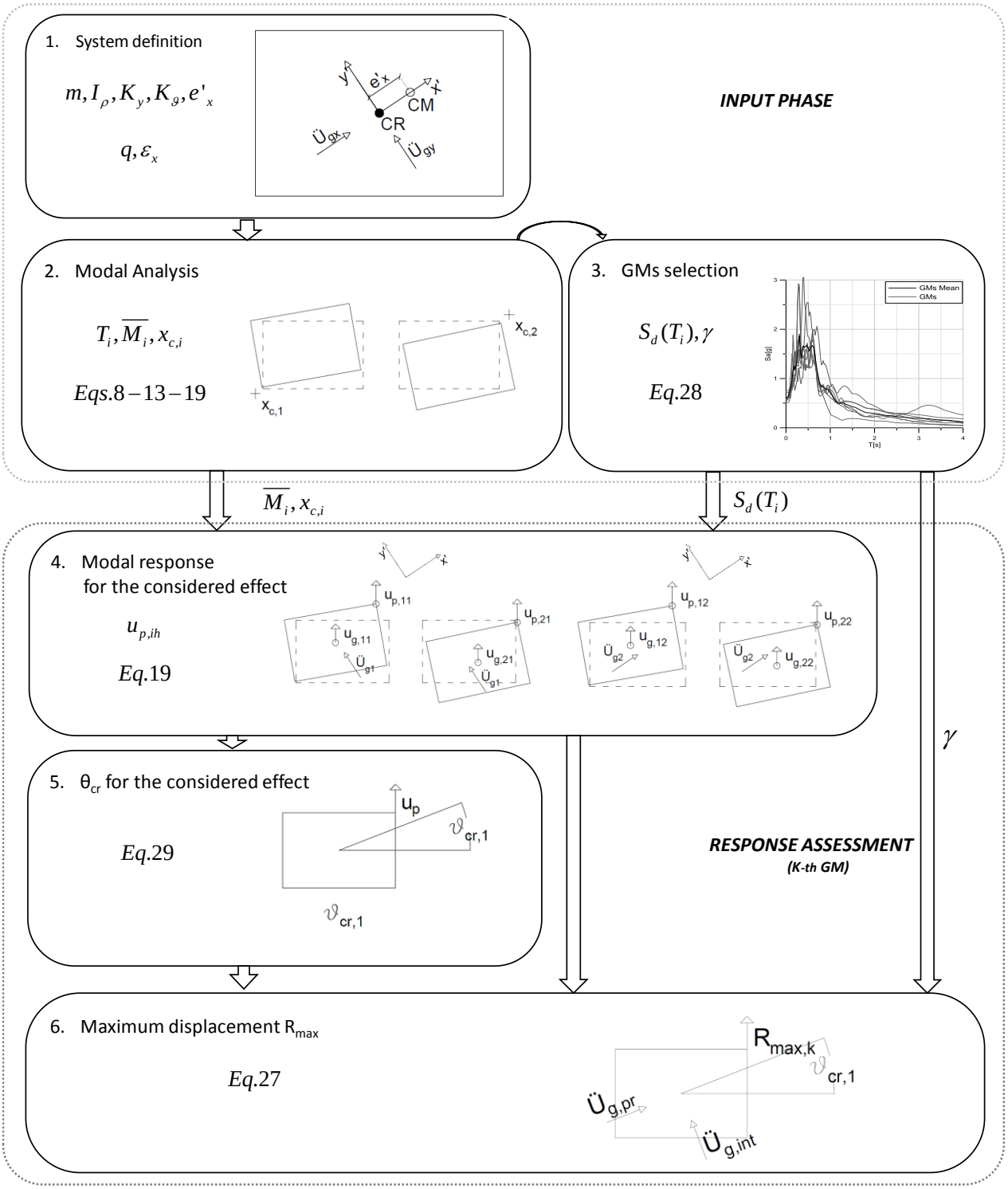

Fig. 6 Flowchart of the proposed procedure

4 CASE STUDY APPLICATIONS

The proposed procedure has been applied to two case studies, a first simpler case study characterized by high regularity, and a second, more complex, which is a real newly designed seismically isolated hospital building in Italy in the site of Lagonegro. The first case study will show and compare the results obtained with monodirectional and bidirectional analyses in order to highlight the main features of the procedure, while the second case study will be used to show the effectiveness of the procedure even in presence of complex seismic isolation systems of irregular structures.

For both case studies the results of the procedure will be compared with dynamic time-history analyses performed with a set of 7 GMs selected for the design of the Lagonegro hospital (Lat 40.13, Lon 15.76). The GM histories have been extracted from a bin of records with a limited interval of magnitude (6<Mw<7.5) and source distance (0<R[km]<40) in order to respect the seismic source properties of the site while, due to the rarity of records with such characteristics, it was not possible to select records with a single fault mechanism. *The selected records have been scaled in order to obtain the spectrum-matching on the code spectrum for a probability of exceedance of 5% in 100 years requested by the Italian code (NTC 2008) for rock soil and then modified to account for local site effects. The scaling factor are chosen in order to obtain the spectrum-matching of the mean spectra of only one component of the selected ground motions records, then the second component is scaled by the same factor in order not to alter the spectral acceleration ratio between horizontal components. Afterwards, each ground motion record has been rotated along the principal axes through the procedure of section §3.1.* The selected records and their properties are shown in Table 1 and Table 2. *It should be emphasized that, due to the use of gagged spectra of natural ground motions, the assessment of γ ratio should be carefully performed because it may significantly change even by considering slightly different periods.*

In the following examples, with the aim of showing the simplest application of the procedure, the γ coefficient in correspondence of the purely translational period of the system is used, however, based on the dynamic characteristics of the various application cases, a γ coefficient assessed in correspondence of other spectral ordinates, or an average coefficient in a significant interval of periods, could be used. Furthermore, some differences in the determination of the γ parameter can be obtained by further manipulation of the accelerograms (such as the use of conditionally simulated ground motions with the use of phase spectra or random phases), however, these evaluations go beyond the scope of this work and are not treated here. In Fig. 7(a) and Fig. 7(b) are shown the records spectra of principal and intermediate components respectively, and in Fig. 7(c) is shown the comparison between the mean spectra of principal and intermediate components. It should be noted that the spectral ordinates of the principal components are significantly higher than the intermediate only for high frequencies (i.e. T<1s) while the two mean spectra are very similar for the spectral ordinates of interest for seismic isolating systems (i.e. T>1s).

Table 1 GMs records characteristics

Database	*Station name*	*Earthquake name*	*Date*	M_w	*Fault mechanism*	*Epicentral distance [km]*	*Waveform*	*PGA[g]*	*EC8 site class*
ESD	Gebze	Izmit (Turkey)	17/08/1999	7.6	strike slip	47	001228XA	0.238	Rock
							001228YA	0.135	
ESD	Izmit	Izmit (Turkey)	17/08/1999	7.6	strike slip	9	001231XA	0.161	Rock
							001231YA	0.224	
ESD	Bingol	Bingol (Turkey)	01/05/2003	6.3	strike slip	14	007142XA	0.497	Rock
							007142YA	0.311	
ESD	Ulcinj	Montenegro	15/04/1979	6.9	thrust fault	5	000198XA	0.18	Rock
							000198YA	0.22	
PEER-NGA	IWT010	Iwate (Japan)	13/06/2008	6.9	reverse	23	5618-EW	0.289	A
							5618-NS	0.226	
PEER-NGA	IZMIT	Kocaeli (Turkey)	17/08/1999	7.5	strike slip	5	1165-090	0.23	A
							1165-180	0.165	
PEER-NGA	VASQUEZ	Northridge (USA)	17/01/1994	6.7	reverse	38	1091-000	0.151	A
							1091-090	0.139	

Table 2 GMs records, rotation angle of principal components, β, scale factors and PGA of scaled principal components

Waveform	β[°]	Principal Components	S.F.	PGA[g]	γ(T=3s)
001228XA	63.08	001228_pr	1.908	0.309	0.647
001228YA		001228_im		0.676	
001231XA	83.63	001231_pr	2.025	0.575	0.788
001231YA		001231_im		0.425	
007142XA	10.29	007142_pr	0.913	0.555	0.605
007142YA		007142_im		0.390	
000198XA	34.91	000198_pr	2.064	0.482	0.934
000198YA		000198_im		0.748	
5618-EW	29.95	5618_pr	1.573	0.552	0.610
5618-NS		5618_im		0.472	
1165-090	5.62	1165_pr	1.972	0.572	0.623
1165-180		1165_im		0.413	
1091-000	88.97	1091_pr	3.006	0.547	0.822
1091-090		1091_im		0.711	

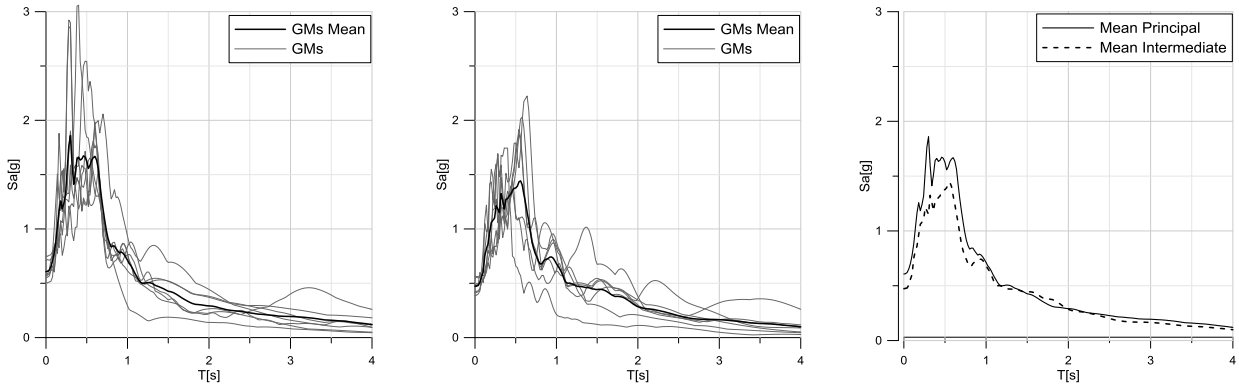

(a) (b) (c)

Fig. 7 GMs spectra of the principal component (a), intermediate components (b), and comparison of mean spectra of principal and intermediate components (c).

4.1 Case study 1, example base isolated structure.

The first case study structure is characterized by a geometric ratio L/B=1, a Torsional factor Ω_s=1, an eccentricity e_x=5%, an equivalent damping ζ_{eq}=10%, and equal stiffness in the X and Y direction with a structural period of translational and rotational mode of the non-eccentric system T=3s. In Fig. 8 is represented the case study 1 with the considered configuration for the position of the center of mass in the case of monodirectional analyses (Fig. 8 left) or bidirectional analyses (Fig. 8 right).

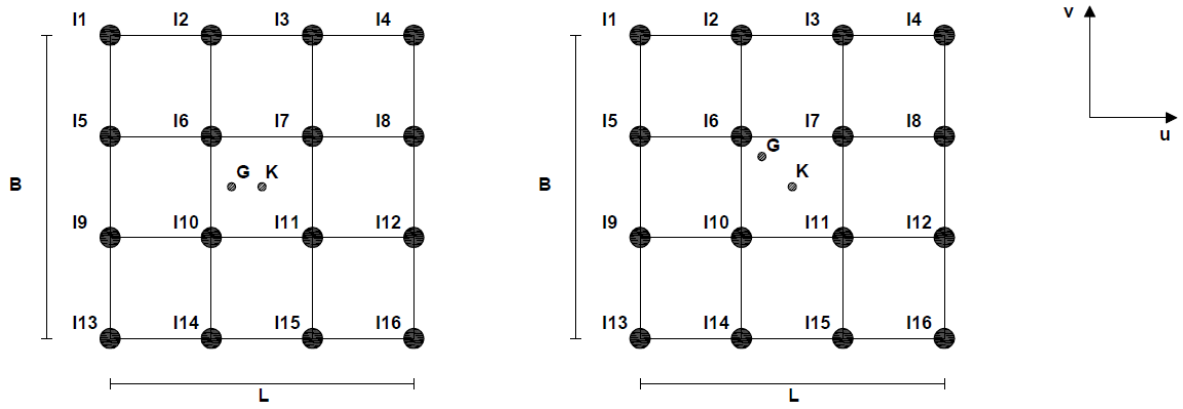

Fig. 8 Representation of case study 1 with eccentricity considered for monodirectional analyses (left) and for bidirectional analyses (right).

A number of time-history analyses have been performed using first only the "principal" components of the GMs set and rotating the records by an interval of 15° in order to change the angle of incidence of the record. The results are compared with those obtained through the Eq. 28 by considering different θ angles and γ=0. The analyses were conducted using Sap2000 (Computers and Structures Inc. 2015), modeling the isolator devices with a linear spring (K=1275kN/m) and a damper (c=1943kN/m). In Fig. 9 are shown the displacements, *u*,in the X-direction (U_{CQC3}) and the displacements, *v*,in the Y-direction (V_{CQC3}) for six different points of the system shown in Fig. 8 (i.e. I1, I2, I4, I13, I14 and I16). A good agreement can be seen between the results of time history analyses and the proposed method, both in terms of absolute values and critical angle of incidence. For the X-direction the maximum displacement is about 30cm for a critical angle of incidence included between -7° and +7°. The displacement in the Y-direction instead, varies significantly from the stiff side of the system (I4 and I16) where it is about 26cm at the flexible side, with maximum displacement over 34cm. By considering that the displacement of the non-eccentric system is 30cm, the observed results are coherent with the maximum amplification factor shown in Fig. 3 which is about 1.15 for L/B=1 ζ=10% and Ω_s=1.

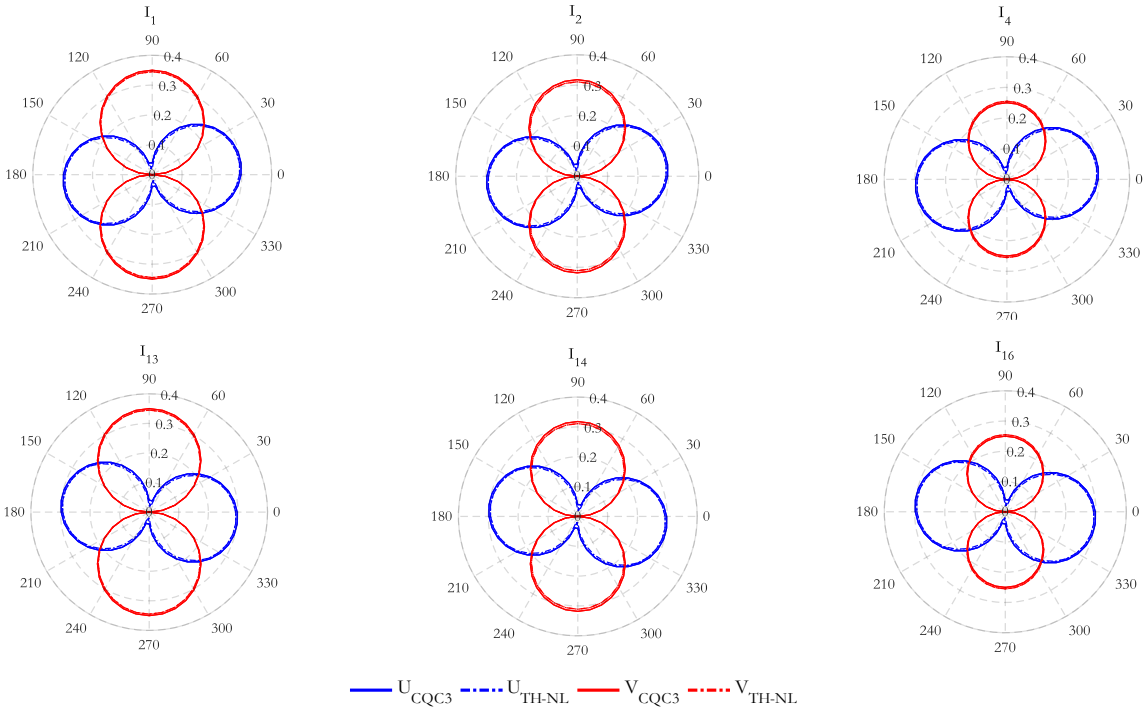

Fig. 9 Directional analyses with single-component earthquake, maximum values of the *u*, *v* displacement components evaluated through CQC3 analyses (solid lines) and compared with results of time history analyses (Dashed lines).

In Fig. 10 are shown the results of bi-directional analyses executed on the case study structure of Fig. 8, by considering a bidirectional earthquake loading and an eccentricity of 5% in both X and Y direction as shown in Fig. 8 right. Both "principal" and "intermediate" records of the set have been used for TH analyses while the γ ratio (evaluated for each couple of records for the pure translational period of the system (i.e. T=3s) (Table 2)) has been used in the Eq. 28 in order to assess the maximum displacement through linear analyses. The results show a good agreement between the two analyses in terms of absolute values, with a maximum displacement of 41.5cm for linear analyses and 42 cm for TH analyses. A slightly difference can be observed about the critical angle of incidence which is zero for linear analyses while it is about 25 degrees for TH analyses.

The parameter of interest for the design of seismic isolation systems is, however, the maximum resultant displacement at each device. In Fig. 10 are shown the values of the maximum vector sum displacements obtained from TH analyses and from the proposed procedure. It can be seen that the proposed method tends to slightly overestimate the maximum displacement of about 15% in almost all the cases, since maximum displacements *u* and *v* computed through linear analyses are not contemporary and their resultant is quite conservative, as already observed in section §2.3, if compared with TH analyses results.

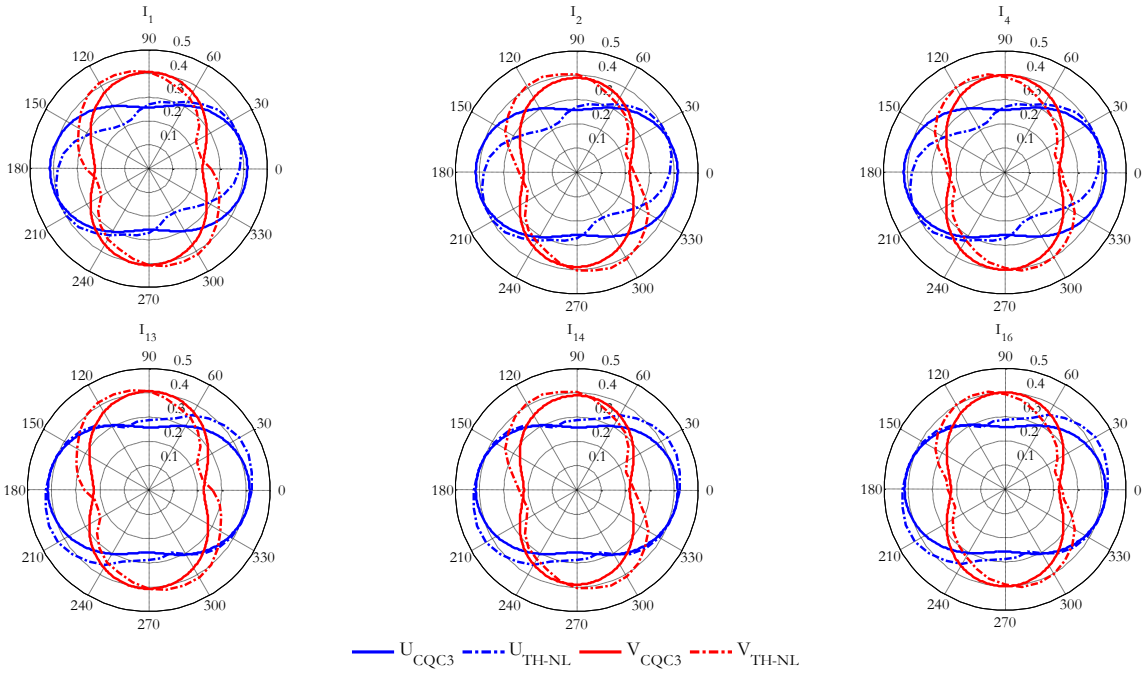

Fig. 10 Directional analyses with two-components earthquake, maximum values of the *u*, *v* displacement components evaluated through CQC3 analyses (solid lines) and compared with results of time history NL (dashed lines)

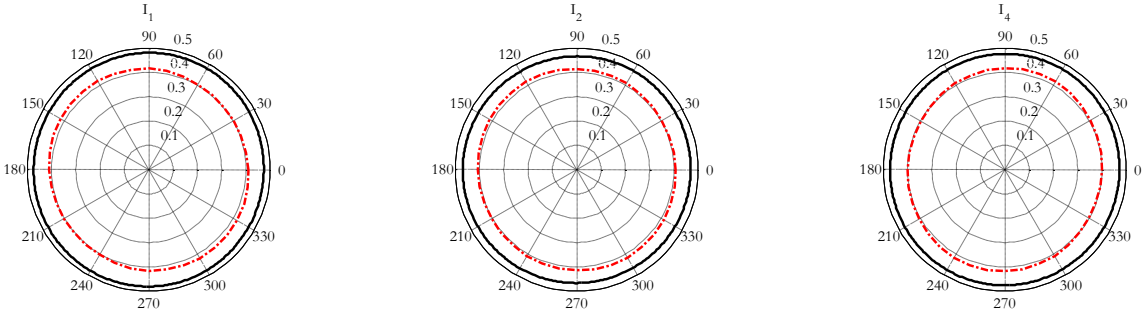

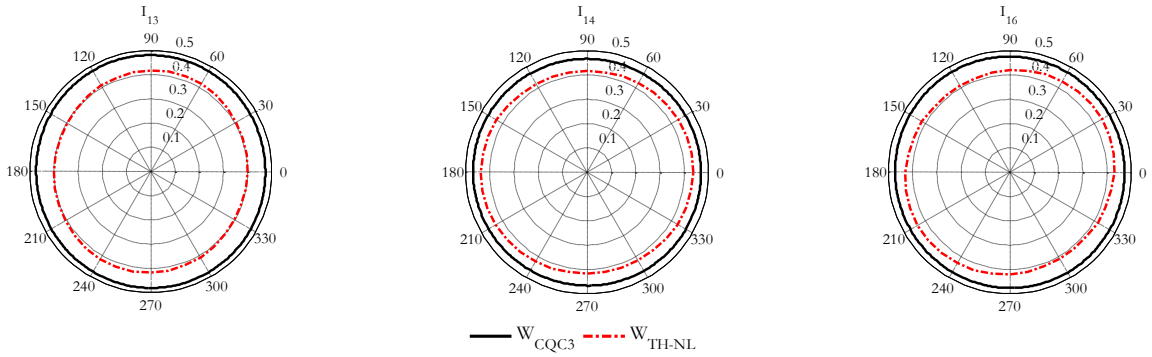

Fig. 11 Maximum resultant displacement *w* obtained through CQC3 combination (solid lines) and nonlinear time history analyses (dashed lines)

4.2 Case study 2, base isolated Lagonegro Hospital, Italy.

This case study is a newly designed isolated structure, intended for hospital use. It is characterized by a significant plan dimension (200x104m at the foundation level) and a number of stories variable from 2 and 8, as shown in Fig. 12 and in Fig. 13 from the transversal section of the Lagonegro hospital building, with max dimension of 112m. The isolation system is characterized by 353 devices of which 247 elastomeric bearing, 53 flat sliders and 53 dissipators, whose plan distribution is shown in Fig. 14. The flat sliders are modeled through a friction element, the dissipators are modeled with an elastoplastic behaviour while the elastomeric bearing are modeled with a viscoelastic model with various stiffness and damping coefficients based on the bearings dimensions, and the characteristics of the different devices adopted are shown in Table 4. The linear equivalent characteristics of the system are shown in Table 3 by considering an action level with a probability of exceedance of 5% in 100 years.

Fig. 12 Longitudinal section of the Lagonegro Hospital building, with max dimension of 200m

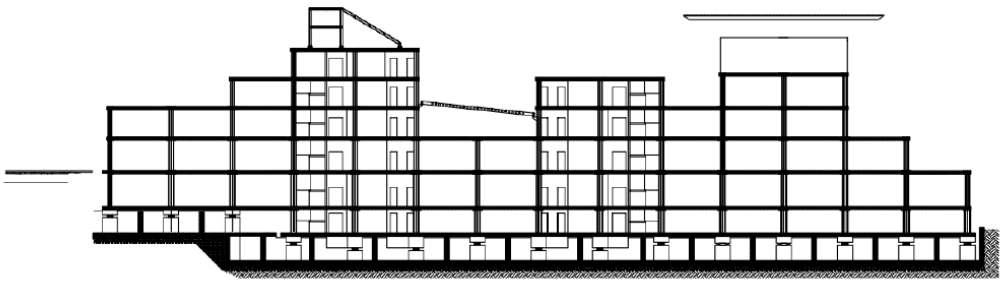

Fig. 13 Transversal section of the Lagonegro hospital building, with max dimension of 112m

Table 3 Lagonegro hospital, total weight of building, W, Period, T_{eq}, Spectral acceleration, $S_e(g)$, Equivalent lateral stiffness, K_{esi}, and equivalent damping, ζ_{esi}, of the isolation system

Total weight of building (kN) W			1115321
Teq(s)	**Se(g)**	**K_{esi} (kN/mm)**	**ξ_{esi}(%)**
2.715	0.142	695.7	21.1

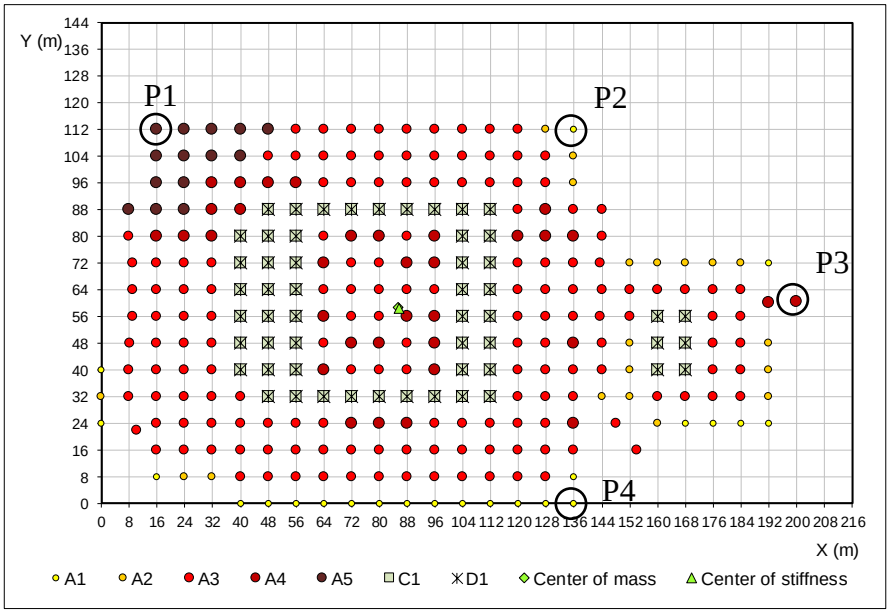

Fig. 14 Plan pattern of devices and response control points of the isolation system

Table 4 Characteristics and modeling parameters for the devices of the seismic isolation system of the Lagonegro hospital building

Tag	*Type*	*K[kN/mm]*	*c[kNs/m]*	*μ[%]*	*F_y[kN]*	*d_y[mm]*
A1	Elastomeric	1.4	136.4	/	/	/
A2	Elastomeric	1.8	154.7	/	/	/
A3	Elastomeric	2.4	178.6	/	/	/
A4	Elastomeric	2.9	196.3	/	/	/
A5	Elastomeric	3.6	218.8	/	/	/
C1	Friction	/	/	2	/	/
D1	Elastoplastic	/	/	/	640	10

For each of the 4 control points shown in Fig. 14 the maximum displacement obtained with the proposed method based on linear analyses is compared with that obtained via Non-Linear (NL) time history analyses. The agreement between the two methods is good for the points P1 and P2 while the simplified method is slightly conservative for the point P3 and P4. Some differences were observed for the P3 point, in particular the simplified method provides a displacement of 34.6cm while the NL analyses gives a maximum displacement of 31.2cm with an overestimate of the first of about 11%.

These results indicate that the proposed method is viable and effective even in the case of a complex structure, due to its good agreement with NL analyses. Further, the overestimation of the maximum displacement compared with NL analyses shown in this case is not higher than the one observed for the simpler case study 1, and in particular, in this case,

with a higher complexity and practice relevance, the overestimate is lower than 10% and practically tolerable for the design purpose.

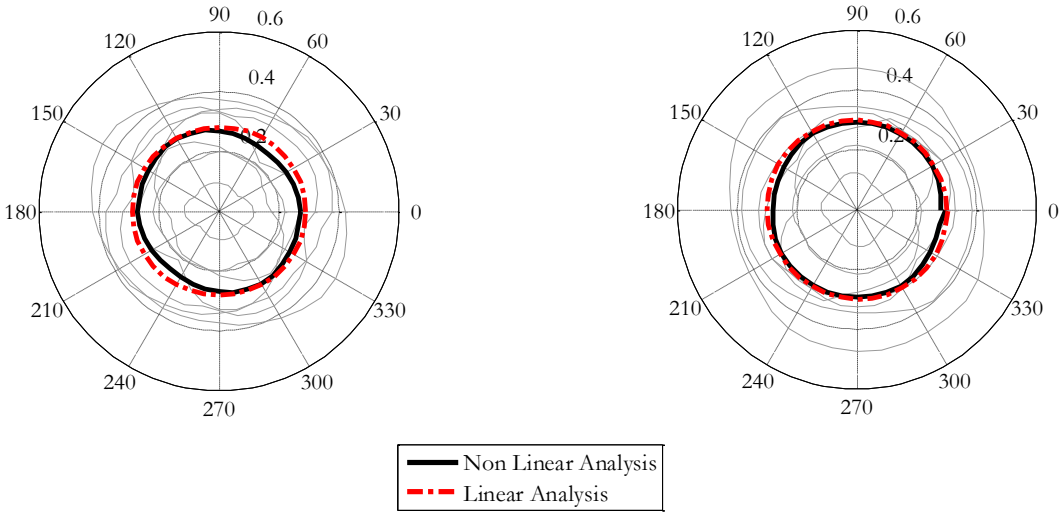

Fig. 15 Maximum resultant displacement obtained through NL dynamic analyses (average) and through the proposed method at the control point P1, (left), and P2 (right)

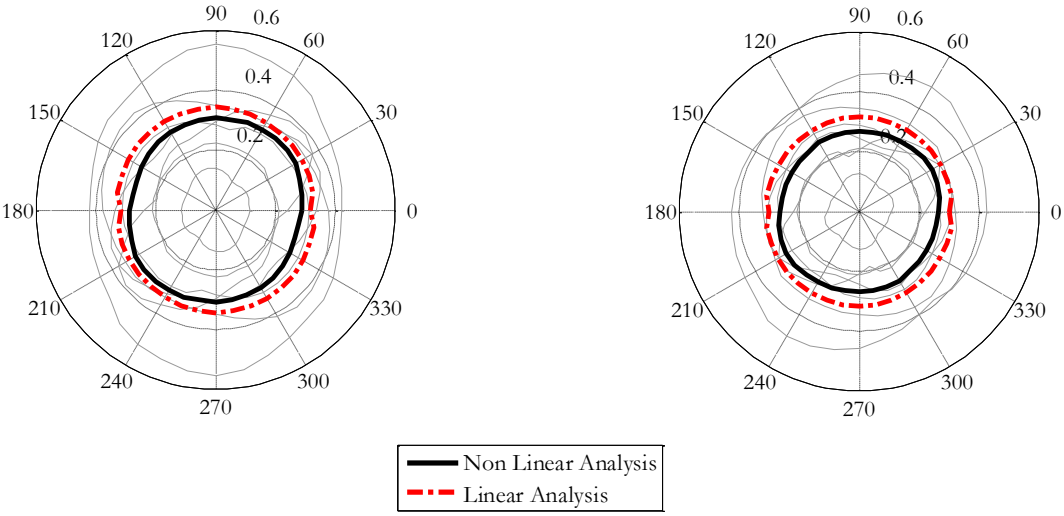

Fig. 16 Maximum resultant displacement obtained through NL dynamic analyses (average) and through the proposed method at the control point P3 (left), and P4 (right)

5 CONCLUSIONS

This work proposed a method for predicting the maximum displacement of seismic isolation systems by using elastic linear analyses and by modeling the seismic action through natural ground motions response spectra. The method allows keeping into account the displacements amplification due to torsional effects by explicitly considering the eccentricity between centers of stiffness and mass in the dynamic response, through a specific representation of the dynamic properties of the system. Based on the CQC3 combination rule for bidirectional earthquake loading, the method allows to properly account for some aspects regarding the seismic action that are commonly neglected, which have a significant importance on the final displacement assessment, such as the directionality effects, by evaluating the critical angle of incidence of

the earthquake, and the specific ratio of ground motion components using natural ground motions response spectra. The comparison with the already available design methods of main international seismic codes show how such methods are often inaccurate, in particular when bi-directional earthquake loading is considered, leading to unrealistic maximum displacement estimates. The comparison of results obtained through TH analyses on case studies has shown a very good agreement in terms of maximum response prediction with the proposed method, both for simple and more complex structures. In particular, for the realistic case study structure of the Lagonegro hospital building, the proposed method leads to a maximum displacement of 11% higher than that obtained via the NL dynamic analyses. In conclusion, the proposed method allows a reliable prediction of maximum displacement demand of seismic isolation systems through simple linear elastic analyses compared to more complex and computationally intensive time history analyses. This features make it useful for design and proportioning seismic isolation systems, providing more accurate predictions compared to current code-based simplified formulations.

6 REFERENCES

ASCE (2010) ASCE/SEI 7-10 Minimum Design Loads for Buildings and other structures. Reston: American Society of Civil Engineers.

Athanatopoulou AM, (2005) Critical orientation of correlated seismic components. Eng. Struct. 27: 301:312.

Baker JW and Allin Cornell C (2006) Spectral shape, epsilon and record selection. Earthq. Eng. Struct. Dyn. 35:1077–1095. doi: 10.1002/eqe.571.

Baker JW and Cornell CA (2006) Which Spectral Acceleration Are You Using? Earthq. Spectra 22:293–312. doi: 10.1193/1.2191540.

Basu D, Constantinou MC and Whittaker AS (2014) An equivalent accidental eccentricity to account for the effects of torsional ground motion on structures. Eng. Struct. 69:1–11. doi: 10.1016/j.engstruct.2014.02.038.

Basu D and Giri S (2015) Accidental eccentricity in multistory buildings due to torsional ground motion. Bull. Earthq. Eng. 13:3779–3808. doi: 10.1007/s10518-015-9788-0.

Basu D, Whittaker AS and Constantinou MC (2015) Characterizing rotational components of earthquake ground motion using a surface distribution method and response of sample structures. Eng. Struct. 99:685–707. doi: 10.1016/j.engstruct.2015.05.029.

Braga F, Faggella M, Gigliotti R and Laterza M (2005) Nonlinear Dynamic Response of HDRB and Hybrid HDRB-Friction Sliders Base Isolation Systems. Bull. Earthq. Eng. 3:333–353. doi: 10.1007/s10518-005-1242-2.

Braga F, Gigliotti R and Laterza M (2009) R/C Existing Structures with Smooth Reinforcing Bars: Experimental Behaviour of Beam-Column Joints Subject to Cyclic Lateral Loads. Open Constr. Build. Technol. J. 3:52–67. doi: 10.2174/1874836800903010052.

Braga F, Gigliotti R and Laguardia R (2019) Intervention cost optimization of bracing systems with multiperformance criteria. Eng. Struct. 182. doi: 10.1016/j.engstruct.2018.12.034.

Calvi GM, Magenes G and Pampanin S (2002) Relevance of Beam-Column Joint Damage and Collapse in Rc Frame Assessment. J. Earthq. Eng. 6:75–100. doi: 10.1080/13632460209350433.

Caprili S, Mattei F, Gigliotti R and Salvatore W (2018) Modified cyclic steel law including bond-slip for analysis of RC structures with plain bars. Earthquakes Struct. 14:187–201. https://doi.org/10.12989/eas.2018.14.3.187

CEN (2004) Eurocode 8: Design of structures for earthquake resistance - Part 1 : General rules, seismic actions and rules for buildings. Eur. Comm. Stand. The European Union Per Regulation 305/2011, Directive 98/34/EC, Directive 2004/18/EC.

Chopra AK and De la Llera JC (1996) Accidental and Natural Torsion in Earthquake Response and Design of Buildings. in Elev. World Conf. Earthq. Eng. Paper No. 2006. Available at: http://www.iitk.ac.in/nicee/wcee/article/11_2006.PDF.

Clough R and Penzien J (1993) Dynamics of structures. McGraw-Hill.

Computers and Structures Inc. (2015) SAP2000 Integrated solution for strucutral analysis & design. Berkeley, California.

Dall'Asta A, Leoni G, Morelli F, Salvatore W and Zona A (2017) An innovative seismic-resistant steel frame with reinforced concrete infill walls. Eng. Struct. Elsevier Ltd 141:144–158. doi: 10.1016/j.engstruct.2017.03.019.

Dicleli M and Buddaram S (2007) Equivalent linear analysis of seismic-isolated bridges subjected to near-fault ground motions with forward rupture directivity effect. Eng. Struct. 29:21–32. doi: 10.1016/j.engstruct.2006.04.004.

Faggella M, Barbosa AR, Conte JP, Spacone E and Restrepo JI (2013) Probabilistic seismic response analysis of a 3-D reinforced concrete building. Struct. Saf. 44:11–27. doi: 10.1016/j.strusafe.2013.04.002.

Faggella M (2014a) Graphic Dynamic Earthquake Response Analysis of Linear Torsionally Coupled 2DOF Systems. in Proc. 9th Int. Conf. Struct. Dyn. Eurodyn. Porto (Portugal) 459–462.
Faggella M (2014b) The Ellipse of Elasticity and Mohr Circle-based graphic dynamic modal analysis of torsionally coupled systems. in Proc. 9th Int. Conf. Struct. Dyn. Eurodyn. Porto (Portugal) 3875–3878.
Faggella M, Gigliotti R, Mezzacapo G and Spacone E (2018) Graphic dynamic prediction of polarized earthquake incidence response for plan‐irregular single story buildings. Bull. Earthq. Eng. 16:4971–5001. doi: 10.1007/s10518-018-0357-1.
Faggella M, Laguardia R, Gigliotti R, Morelli F, Braga F, Salvatore W (2016) Performance-based nonlinear response history analysis framework for the "PROINDUSTRY" project case studies. ECCOMAS Congress 2016 – Proce. of the 7th European Congress on Computational Methods in Applied Sciences and Engineering Volume 3, 2016, Pages 5912-5925, Crete; Greece; 5-10 June 2016.
Faggella M, Gigliotti R, Morrone C and Spacone E (2017). Mohr Circle-based Graphical Vibration Analysis and Earthquake Response of Asymmetric Systems. Procedia Engineering Volume 199, 2017, 10th International Conference on Structural Dynamics, EURODYN 2017, Pages 128-133
Formisano A, De Matteis G, Panico S and Mazzolani FM (2008) Seismic upgrading of existing RC buildings by slender steel shear panels: A full-scale experimental investigation. Adv. Steel Constr. 4:26–45.
Formisano A and Massimilla A (2018) A Novel Procedure for Simplified Nonlinear Numerical Modeling of Structural Units in Masonry Aggregates. Int. J. Archit. Herit. Taylor & Francis 12:1162–1170. doi: 10.1080/15583058.2018.1503365.
Jangid RS and Kelly JM (2000) Torsional Displacements in Base Isolated Buildings. Earthq. Spectra 16:443–454.
Jangid RS and Kelly JM (2001) Base isolation for near-fault motions. Earthq. Eng. Struct. Dyn. 30:691–707. doi: 10.1002/eqe.31.
Kelly JM (1999) The role of damping in seismic isolation. Earthq. Eng. Struct. Dyn. 28:3–20. doi: 10.1002/(SICI)1096-9845(199901)28:1<3::AID-EQE801>3.0.CO;2-D.
Kohrangi M, Bazzurro P and Vamvatsikos D (2016) Vector and scalar IMs in structural response estimation, Part I: Hazard analysis. Earthq. Spectra 32:1507–1524. doi: 10.1193/053115EQS080M.
Koren D, Kilar V, (2011) The applicability of the N2 method to the estimation of torsional effects in asymmetric base-isolated buildings. Earthq. Eng. Struct. Dyn. 2011; 40: 867-886. DOI: 10.1002/eqe.1064.
Laguardia R, Gigliotti R and Braga F (2017) Optimal design of dissipative braces for seismic retrofitting through a multi-performance procedure. in Seism. Eng. Italy ANIDIS 2017. Pistoia.
Laterza M, D'Amato M, Braga F and Gigliotti R (2017a) Extension to rectangular section of an analytical model for concrete confined by steel stirrups and/or FRP jackets. Compos. Struct. 176:910–922. doi: 10.1016/j.compstruct.2017.06.025.
Laterza M, D'Amato M and Gigliotti R (2017) Modeling of gravity-designed RC sub-assemblages subjected to lateral loads. Eng. Struct. 130:242–260. doi: 10.1016/j.engstruct.2016.10.044.
López OA and Torres R (1997) The critical angle of seismic incidence and the maximum structural response. Earthq. Eng. Struct. Dyn. 26:881–894. doi: 10.1002/(SICI)1096-9845(199709)26:9<881::AID-EQE674>3.0.CO;2-R.
Lu LY and Lin GL (2009) Improvement of near-fault seismic isolation using a resettable variable stiffness damper. Eng. Struct. 31:2097–2114. doi: 10.1016/j.engstruct.2009.03.011.
Menun C and Der Kiureghian A (1998) A replacement for the 30%, 40%, and SRSS rules for multicomponent seismic analysis. Earthq. Spectra 153–163. doi: 10.1193/1.1586025.
Mohammad AF, Faggella M, Gigliotti R and Spacone E (2016) Seismic performance of older R/C frame structures accounting for infills-induced shear failure of columns. Eng. Struct. 122:1–13. doi: 10.1016/j.engstruct.2016.05.010.
Mohammad AF, Faggella M, Gigliotti R and Spacone E (2018). "Effects of Bond-Slip and Masonry Infills Interaction on Seismic Performance of Older R/C Frame Structures". Soil Dynamics and Earthquake Engineering. https://doi.org/10.1016/j.soildyn.2018.02.027.
Morelli F, Piscini A and Salvatore W (2017) Seismic behavior of an industrial steel structure retrofitted with self-centering hysteretic dampers. J. Constr. Steel Res. 139:157–175. doi: 10.1016/j.jcsr.2017.09.025.
Morelli F, Laguardia R, Faggella M, Piscini A, Gigliotti R and Salvatore W (2018) Ground motions and scaling techniques for 3D performance based seismic assessment of an industrial steel structure. Bull. Earthq. Eng. 16:1179–1208. doi: 10.1007/s10518-017-0244-1.
Nagarajaiah S, Reinhorn A and Constantinou M (1993) Torsion in Base-Isolated structures with elastomeric isolation systems. J. Struct. Eng. 119:2932–2951.
NTC (2008) Norme tecniche per le costruzioni D.M. 14 Gennaio 2008. Edited by Italian ministry of Infrastructure. Rome (IT): Gazzetta Ufficiale n. 29 of february 4th 2008 - Suppl. Ordinario n. 30. In Italian.
NTC (2018) D.M. 17.01.18 Aggiornamento delle 'Norme Tecniche per le costruzioni'. Edited by Italian Ministry of Infrastructure. Rome: Italian Ministry of Infrastructure.
Palermo M, Gasparini G, Silvestri S and Trombetti T (2013) The maximum corner displacement magnification of one-storey eccentric systems. Bull. Earthq. Eng. 11:1467–1491. doi: 10.1007/s10518-013-9445-4.
Pant DR, Constantinou MC and Wijeyewickrema AC (2013) Re-evaluation of equivalent lateral force procedure for prediction of displacement demand in seismically isolated structures. Eng. Struct. 52:455–465. doi:

10.1016/j.engstruct.2013.03.013.
Penzien J and Watabe M (1974) Characteristics of 3- dimensional earthquake ground motions. Earthq. Eng. Struct. Dyn. 3:365–373. doi: 10.1002/eqe.4290030407.
Rezaeian S and Der Kiureghian A (2010) Stochastic Modeling and Simulation of Near-Fault Ground Motions for Performance-Based Earthquake Engineering. Pacific Earthq. Eng. Res. Cent.
Roussis PC, Tsopelas PC and Constantinou MC (2013) Nonlinear dynamic analysis of multi-base seismically isolated structures with uplift potential II: verification examples. Earthq. Eng. Eng. Vib. 9:83–91. doi: 10.1007/s11803-010-9047-y.
Ryan KL and Chopra AK (2004) Estimation of Seismic Demands on Isolators Based on Nonlinear Analysis. J. Struct. Eng. 130:392–402. doi: 10.1061/(ASCE)0733-9445(2004)130:3(392).
Smeby W and der Kiureghian A (1985) Modal combination rules for multicomponent earthquake excitation. Earthq. Eng. Struct. Dyn. 13:1–12. doi: 10.1002/eqe.4290130103.
Somerville P (1998) Development of an improved representation of near fault ground motions. SMIP98 Semin. Util. Strong-Motion Data 1–20. Available at: http://www.conservation.ca.gov/cgs/smip/docs/seminar/SMIP98/Documents/SMIP98_Proceedings.pdf#page=11.
Tena-Colunga A and Escamilla-Cruz JL (2007) Torsional amplifications in asymmetric base-isolated structures. Eng. Struct. 29:237–247. doi: 10.1016/j.engstruct.2006.03.036.
Tena-Colunga A and Zambrana-Rojas C (2006) Dynamic torsional amplifications of base-isolated structures with an eccentric isolation system. Eng. Struct. 28:72–83. doi: 10.1016/j.engstruct.2005.07.003.
Trombetti T, Silvestri S, Gasparini G, Pintucchi B and De Stefano M (2008) Numerical Verification of the Effectiveness of the "Alpha" Method for the Estimation of the Maximum Rotational Elastic Response of Eccentric Systems. J. Earthq. Eng. doi: 10.1080/13632460701385374.
Trombetti TL and Conte JP (2005) New insight into and simplified approach to seismic analysis of torsionally coupled one-story, elastic systems. J. Sound Vib. 286:265–312. doi: 10.1016/j.jsv.2004.10.021.
Warn GP and Whittaker AS (2004) Performance estimates in seismically isolated bridge structures. Eng. Struct. 26:1261–1278. doi: 10.1016/j.engstruct.2004.04.006.
Wilson EL, Der Kiureghian A and Bayo P (1981) A Replacement for the SRSS Method in Seismic Analysis. Earthq. Eng. Struct. Dyn. 9:187–194.
Wolff ED, Ipek C, Constantinou MC and Morillas L (2014) Torsional response of seismically isolated structures revisited. Eng. Struct. 59:462–468. doi: 10.1016/j.engstruct.2013.11.017.